Ultrafast optical switching to a metallic state via photoinduced Mott transition in few-layer MoS_2 under hydrostatic pressure

Qingyi Li,[1,2] Laizhi Sui,[2,*] Guangming Niu,[2,3] Jutao Jiang,[2] Yutong Zhang,[2] Li Che,[3] Guorong Wu,[2] Mingxing Jin,[1,†] and Kaijun Yuan[2,‡]

[1]*Institute of Atomic and Molecular Physics, Jilin Provincial Key Laboratory of Applied Atomic and Molecular Spectroscopy, Jilin University, Changchun, 130012, People's Republic of China*

[2]*State Key Laboratory of Molecular Reaction Dynamics, Dalian Institute of Chemical Physics, Chinese Academy of Sciences, Dalian, 116023, People's Republic of China*

[3]*College of Science, Dalian Maritime University, Dalian, 116026, People's Republic of China*

(Received 6 September 2020; accepted 3 March 2021; published 16 March 2021)

Photoinduced Mott transition has been revealed as a superior method to control the optical and electronic properties in excited semiconductors on ultrashort timescales but the corresponding ultrafast carrier dynamics and the underlying many-body interactions, together with their responses to external stimuli besides optical excitation, are still poorly understood. Herein, we experimentally demonstrate that the photoinduced Mott transition in few-layer MoS_2 at room temperature can be achieved and subtly tuned under mild optical excitation via hydrostatic pressure. Utilizing ultrafast pump-probe spectroscopy, significant reduction of the Mott density by more than two orders of magnitude and a gradual acceleration of the optical switching to the metallic electron-hole plasma state under elevated pressures up to ∼3 GPa are experimentally revealed, which can be attributed to the reduction of the exciton binding energy and the acceleration of the exciton dissociation under hydrostatic pressure.

DOI: 10.1103/PhysRevB.103.125416

I. INTRODUCTION

The study and control of many-body interactions between charge carriers, which govern the electronic properties and optical responses of excited semiconductors, are of pivotal importance in condensed-matter physics [1]. Under low optical excitation, bound electron-hole pairs, or excitons, can be formed via Coulomb interactions in semiconductors and quantum wells [2–4]. With the increase of the charge carrier density beyond the so-called Mott density, insulating excitons will dissociate due to the screening of the Coulomb interactions and transform into an exotic electron-hole plasma phase [5–7]. Since the plasma phase exhibits unique metallic conductivity, this nonequilibrium phase transition is often referred to as a photoinduced Mott transition [8–10]. Due to the significant exciton dissociation and band-gap renormalization, spectral features like exciton energy shifts are accompanied. Based on these features, the Mott transition together with the Mott density can thus be defined and demonstrated in this paper.

The thermodynamic balance of the transition between excitons and electron-hole plasma in excited semiconductors can be described by the scheme of ionization equilibrium [11]. According to a recent theoretical study [12], this thermodynamic balance can be efficiently tuned via means like dielectric engineering as well as charge carrier doping, which triggers the motivation for the experimental study and control of the optoelectronic properties and phase transitions in semiconductors via photoinduced Mott transition. In this context, the emergence of two-dimensional (2D) semiconducting transition-metal dichalcogenides (TMDCs) provides great opportunities to achieve this goal experimentally [13,14]. Owing to the strong quantum confinement and the greatly reduced dielectric screening, Coulomb interactions in atomically thin TMDCs are significantly enhanced, which results in tightly bound excitons with binding energy of several hundreds of meV that dominate the optical response as pronounced resonances [15–20]. These advantages lay the foundation for the study of exciton-related many-body interactions and strong-correlation effects in atomically thin TMDCs via spectroscopic methods at room temperature [21–26]. Utilizing ultrafast pump-probe spectroscopy, photoinduced Mott transition accompanied by the development of population inversion in mono and bilayer WS_2 under pump fluences of several mJ/cm^2 at room temperature has been explored [27], which indicates the promising application of TMDCs in the construction of nanolasers [28–31]. Meanwhile, the significant changes in the optical response after excitation are found to be highly transient with lifetimes of the metallic state on the picosecond timescale, which reveals that the photoinduced Mott transition in atomically thin TMDCs could be exploited to build new types of ultrafast optical switches [9,32].

In practical optoelectronic applications, various external stimuli, such as temperature, pressure, or magnetic fields, can significantly affect the device performance besides

*lzsui@dicp.ac.cn
†mxjin@jlu.edu.cn
‡kjyuan@dicp.ac.cn

illumination. Owing to the weak van der Waals interlayer interactions, a few-layer TMDC semiconductor like MoS_2 is extremely sensitive to external compression strain [33]. Meanwhile, with remarkably strong mechanical strength in the monolayer limit, atomically thin TMDCs can withstand ultrahigh external pressure [34]. As a clean and nonintrusive strain-engineering approach, hydrostatic pressure generated by a diamond anvil cell (DAC) is able to impose ultrahigh and reversible compression strain without breaking the sample, which makes it a potential and widely used mechanical method in the modulation of structural, electronic, and optical properties of 2D nanomaterials like TMDC semiconductors [35,36]. However, though a number of studies have addressed the optical properties and electronic structures of TMDCs under pressure in the steady state [37–45], systematic investigations of the influence from the pressure on nonequilibrium phase transition and the underlying many-body interactions between photogenerated charge carriers are still lacking.

Here, utilizing the broadband femtosecond TA spectroscopy combined with DAC devices [46], we experimentally demonstrate that the photoinduced Mott transition in few-layer MoS_2 at room temperature can be achieved and subtly tuned under low excitation density via hydrostatic pressure. First, we show that the variations of the optical response of the sample under elevated pump fluences, especially the relative energy shifts of the lowest exciton resonance (A exciton) in the absorption spectra of MoS_2, reflect directly the evolution of ionization equilibrium between excitons and electron-hole plasma at the Mott transition. Based on analyses of these critical behaviors, a Mott density of $\sim 4.2 \times 10^{13}/\mathrm{cm}^2$ of the sample under ambient pressure is derived, which is in good agreement with previous studies [19,27]. Under pressure of around 3 GPa, the Mott density is significantly reduced by more than two orders of magnitude. As the pressure increases from 2.00 to 3.25 GPa, the time needed for the ultrafast establishment of the metallic electron-hole plasma state after excitation is successively reduced from 5.8 to 2.9 ps with an almost linear acceleration of the corresponding transition rate, which is ascribed to the reduction of the exciton binding energy and the acceleration of the exciton dissociation via the enhanced dielectric screening of the Coulomb interactions by the pressure.

II. RESULTS AND DISCUSSION

The sample of the few-layer MoS_2 was prepared via liquid-phase exfoliation [47], which possesses an average thickness of ~2 nm and corresponds to 2–3 layers with sample characterization using atomic-force microscopy topography (see Fig. S1 in the Supplemental Material [48]). Throughout the TA experiments at room temperature, femtosecond laser pulses with a duration of 35 fs at 400 nm were utilized as the pump, which deliver a single photon energy of 3.10 eV that is much higher than the quasiparticle band gap of ~2.4 eV in atomically thin MoS_2 [18]. White light supercontinuum pulses with a spectral range from ~420 nm to 800 nm were used as the probe, where the pump and the probe pulses are colinearly polarized. Without the pump excitation, the linear absorption spectrum of the few-layer MoS_2 is dominated by the A and B exciton resonances, which originate from the direct transition at the K and K′ points in the first Brillouin zone with energies of around 1.85 and 2.01 eV, respectively [15]. At time delay of 2 ps after the pump excitation, the absorption spectra of the A exciton in few-layer MoS_2 under a series of pump fluences from 17.7 to 707 $\mu\mathrm{J}/\mathrm{cm}^2$ are measured, and the resultant energy shifts of the exciton resonance energy as a function of the pump fluence are shown in Fig. 1. Note that the MoS_2 dispersion is highly transparent and uniform, then the reflection or scattering of the probe can be neglected, and thus the measured absorbance A [or optical density (OD)] mainly comes from the absorption of the probe by the sample.

Upon excitation, hot carriers are pumped from the valence band up to the conduction band, which cool down to the band edge in few-layer MoS_2 on subpicosecond timescales [23]. Therefore, at time delay of 2 ps, hot carrier cooling has already finished, while the recombination of electron-hole pairs has not yet happened, which ensures the rationality for the study of excitons at 2 ps. In Figs. 1(a) and 1(b), the rise and decline of redshift of the A exciton absorption peak in few-layer MoS_2 with the increase of the pump fluence under ambient pressure are shown, and the corresponding exciton resonance energy shift (ΔE) as a function of the pump fluence (excitation density) is shown in Fig. 1(c). When the pump fluence is lower than 62.5 $\mu\mathrm{J}/\mathrm{cm}^2$, the A exciton resonance energy gradually redshifts for ~9 meV with the increase of the excitation density. When the elevated pump fluence exceeds 62.5 $\mu\mathrm{J}/\mathrm{cm}^2$, however, a remarkable declining redshift occurs for the A exciton resonance energy, which shares similarity with the findings in a previous experimental study on monolayer WS_2 [49]. It is well known that the measured exciton resonance energy actually reflects the energy difference between the quasiparticle band gap and the related exciton binding energy [50]. Upon optical excitation, efficient tuning of both the exciton binding energy and quasiparticle band gap due to the dynamical screening of the Coulomb interactions from the photogenerated electron-hole pairs and free carriers have been observed in atomically thin TMDC semiconductors [51]. Basically, with the increase of the electron-hole excitation density, one consequence from the dynamical screening of the Coulomb interactions is the decrease of the so-called self-energy contribution, which can be used to quantify the repulsive interactions between identical charges. The decrease of self-energy will then lead to a reduction of the quasiparticle band gap, which is called the photoinduced band-gap renormalization [27,51–53]. In addition, with the increase of the exciton and free carrier density, the screening of the attractive interactions in electron-hole pairs will result in a further reduction of the exciton binding energy and facilitate exciton dissociation [12,51]. The competition between these two effects eventually leads to the shifts of the exciton resonance energy.

According to the theoretical study of the ionization equilibrium between excitons and electron-hole plasma in TMDCs [12], when the electron-hole excitation density is lower than the Mott density, the ionization equilibrium will be dominated by the excitons. Under this circumstances, the dipolar screening from the excitons will result in prominent band-gap renormalization, leading to a redshift of the exciton resonance energy. With further increase of the excitation density above the Mott threshold, the dominance of

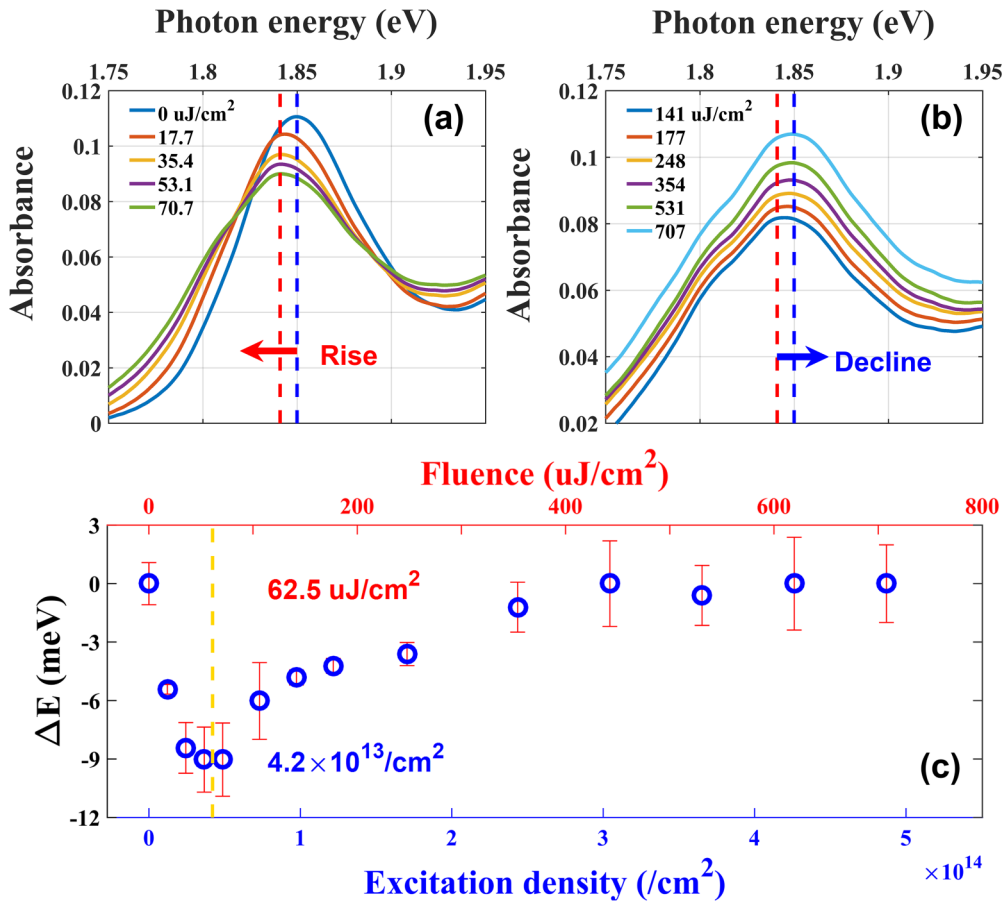

FIG. 1. The (a) rise and (b) decline of redshift of the A exciton absorption spectra in few-layer MoS_2 under ambient pressure with the increase of the pump fluence, respectively. The corresponding time delay is fixed at 2 ps. In both panels, two vertical dashed lines are shown to highlight the initial (blue) and the maximal redshift (red) of the A exciton resonance peak position. (c) Relative energy shifts of the A exciton resonance energy in few-layer MoS_2 under ambient pressure as a function of the pump fluence or electron-hole excitation density. The yellow vertical dashed line is shown to highlight the observed rise and decline of redshift of the A exciton together with the corresponding pump fluence of around 62.5 $\mu J/cm^2$ and electron-hole excitation density of $4.2 \times 10^{13}/cm^2$.

the ionization equilibrium will be transferred from the excitons to the electron-hole plasma, which is accompanied by a significant reduction of the exciton binding energy and efficient dissociation of the insulating excitons into metallic electron-hole plasma. Once the decrease of the exciton binding energy becomes larger than that of the band-gap renormalization, a declining redshift of the exciton resonance energy is expected. Within this context, the rise and decline of redshift shown in Fig. 1(c) can be attributed to the onset of the photoinduced Mott transition in few-layer MoS_2 at the pump fluence of around 62.5 $\mu J/cm^2$. Note that the transition happens roughly at a ten times increased pump fluence in our experiment compared to that in Ref. [49], where monolayer WS_2 was experimentally studied at room temperature. Generally speaking, the onset of exciton Mott transition (EMT) sets in when the screening length due to excitons and free carriers becomes comparable to or less than the Bohr radius of the bound exciton. Different from the monolayer condition where excitons are spatially confined in the single layer, more bound excitons can be held before EMT in few-layer TMDCs with spare layers. In return, more injected electron-hole pairs are needed to fulfill the requirements for EMT, which should be the leading cause of the much higher pump fluence found in our experiment. Considering the absorbance of the sample at the pump wavelength, the corresponding electron-hole excitation density is estimated to be $4.2 \times 10^{13}/cm^2$ (see the Supplemental Material [48] for details), which is in agreement with previously reported values of Mott density in atomically thin TMDCs [19,27].

To get a deeper insight into the ultrafast optical responses of few-layer MoS_2 around the Mott transition under ambient pressure, series of selected TA spectra of the A exciton with the increase of the pump fluence from 17.7 to 707 $\mu J/cm^2$ are presented in Fig. 2 (the corresponding TA spectra with full spectral range of the probe are shown in Figs. S3 and S4 in the Supplemental Material [48]). In our TA experiment, each measurement under a certain pump fluence or hydrostatic pressure was repeated at least ten times to sufficiently reduce the system error, which leads to smooth TA spectra as shown in Figs. 2 and 3. Here the main x axis of wavelength scale was adopted to exhibit the TA spectra from 620 nm to 730 nm, and an additional x axis on top was also shown to provide the corresponding energy scale as a reference. The y axis $\Delta OD = OD_{\text{pump on}} - OD_{\text{pump off}}$ represents the difference of the absorbance or OD of the probe with the pump on/off,

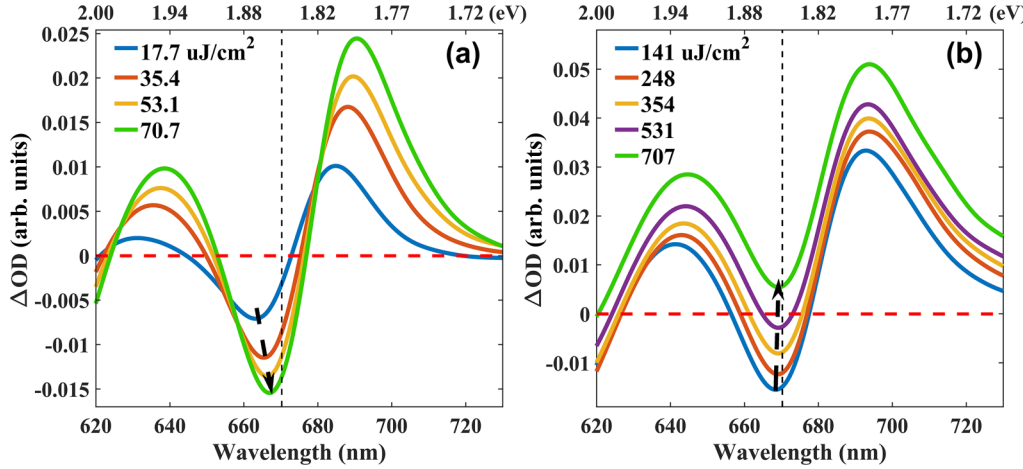

FIG. 2. The variation of TA spectra of the A exicton in few-layer MoS_2 with the increase of the pump fluence (a) below and (b) above the Mott threshold under ambient pressure, the spectra are taken at fixed time delay of 2 ps at room temperature. The vertical dashed lines indicate the A exciton energy without the pump excitation.

which delivers information of TA behavior of the sample at certain time delay after the excitation of the pump. The TA spectra in Fig. 2 are taken at time delay of 2 ps, which share common spectral features with a negative peak at around 660–670 nm surrounded by two positive peaks. From previous studies, it is known that the negative peak represents the signal of ground state bleaching of the A exciton which dominates the steady-state absorption spectrum in few-layer MoS_2 [15], while the positive signal on the low energy side is claimed to be related to the excited state absorption of charged excitons (trions) or biexcitons [54–58].

As shown in Fig. 2(a), the intensity of the A exciton bleaching peak is significantly enhanced with the increase of the pump fluence from 17.7 to 70.7 $\mu J/cm^2$. With the further increase of the pump fluence beyond the Mott threshold, different variation tendencies of the TA spectra are shown in Fig. 2(b). On the one hand, an unexpected decrease of the intensity of the negative bleaching peak occurs as the pump fluence increases from 141 to 531 $\mu J/cm^2$, which reflects a successive rising of the whole spectrum. Strikingly, the whole spectrum eventually evolves into an overall positive signal, together with the survival of the exciton bleaching peak as a valley against the positive background under the pump fluence of 707 $\mu J/cm^2$ ($4.7 \times 10^{14}/cm^2$) (see the corresponding TA spectra at selected time delays under pump fluence of 70.7 and 707 $\mu J/cm^2$ in Fig. S5 and S6 in the Supplemental Material). On the other hand, a relatively slow but steady broadening of the linewidth of the exciton bleaching peak arises with the increase of the pump fluence beyond the Mott threshold. Upon the excitation density above the Mott threshold, the ionization equilibrium will be transferred from the excitons to the electron-hole plasma. In other words, the photogenerated electron-hole pairs tend to exist as free charge carriers rather than excitons under intense optical excitation above the Mott density. Meanwhile, the exciton dissociation will also be enhanced. Therefore, the intensity decrease of the exciton bleaching peak and the successive rising of the whole spectrum, which eventually manifests itself as a positive signal after sign reversal shown in Fig. 2(b), could be attributed to the enhanced exciton dissociation and the broad and growing positive absorption signal of the free charge carriers at elevated excitation densities beyond the Mott threshold, whereas the overall linewidth broadening of the exciton bleaching peak is a natural result of the exciton fission together with the enhanced carrier-carrier and carrier-phonon scattering. Note that the exciton signal here survives beyond the Mott transition even under pump fluence of 707 $\mu J/cm^2$, which is more than ten times larger than the corresponding pump fluence of 62.5 $\mu J/cm^2$ of the Mott density. As a reasonable explanation, the Coulomb or excitonic enhancement effect could be adopted [59], which refers to the persistence of excitons in an electron-hole plasma due to the remaining correlation effects even above the Mott transition [60–62]. These findings may provide a direct ultrafast spectroscopic proof for the theoretical studies on the ionization equilibrium between excitons and electron-hole plasma in TMDC semiconductors [12].

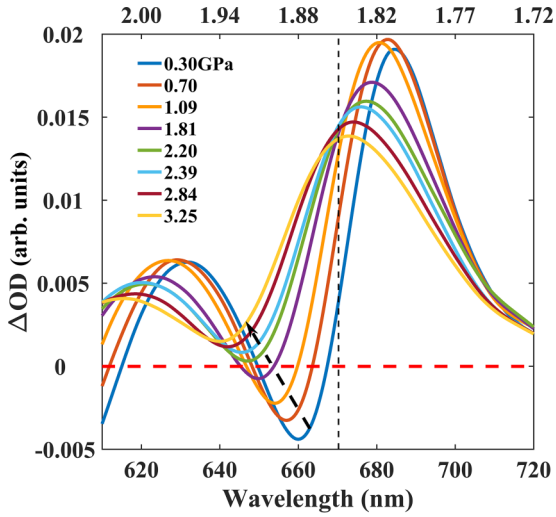

FIG. 3. The variation of TA spectra of the A exciton in few-layer MoS_2 with the increase of the hydrostatic pressure from 0.30 to 3.25 GPa under low excitation density of $3.29 \times 10^{12}/cm^2$ (5.64 $\mu J/cm^2$), the TA spectra are taken at time delay of 7 ps at room temperature.

With the aim to further investigate the response of the concerned nonequilibrium phase transition to external strain, we then conducted TA measurements of few-layer MoS_2 under hydrostatic pressure with fixed pump fluence, and the details of the experimental setup can be found in the Supplemental Material [48]. To our surprise, the above-mentioned spectral feature of sign reversal of the A exciton bleaching peak from negative to positive under strong excitation at ambient pressure was also found under high pressure above 1.81 GPa with only mild excitation. Specifically, the sign reversal in TA spectrum first arose under pressure of 2.00 GPa at time delay of around 6 ps. With further increase of the pressure, the concerned sign reversal always occurred. Meanwhile, the higher the pressure was, the faster the sign reversal arose. To show the evolution of the TA spectra with special emphasis on the positive ones shortly after the sign reversal, in Fig. 3, a series of selected TA spectra of few-layer MoS_2 with the increase of pressure from 0.30 to 3.25 GPa are presented at a time delay of 7 ps.

The elimination of the influence from optical excitation is a prerequisite for a reasonable discussion of the influences induced solely by the hydrostatic pressure. To this end, a careful examination of the absorbance of the few-layer MoS_2 sample at the excitation wavelength of 400 nm under different pressures has been conducted using steady-state absorption spectroscopy, and the results are presented in Fig. S2 (see Fig. S2 in the Supplemental Material [48]). In contrast to the significant blueshift and gradual weakening of the exciton resonances, the absorbance at the excitation wavelength remains almost unchanged under elevated hydrostatic pressures (Fig. S2). The final electron-hole excitation density at the sample inside the DAC cavity is estimated to be $\sim 3.29 \times 10^{12}/\mathrm{cm}^2$ (see the Supplemental Material [48] for details), which is maintained throughout the TA measurements under hydrostatic pressure. Since this excitation density ($3.29 \times 10^{12}/\mathrm{cm}^2$) is an order of magnitude lower than the Mott density ($4.2 \times 10^{13}/\mathrm{cm}^2$) of the few-layer MoS_2 at ambient pressure, the Mott transition should not be able to occur under relatively low pressures, which is evidenced by the overall similarity between the initial TA spectra in Fig. 3 below 1.09 GPa and those shown in Fig. 2(a) under ambient pressure.

Following the black dashed arrow in Fig. 3, successive blueshift of the TA spectra especially for the bleaching peak of A exciton with the increase of the hydrostatic pressure can be observed, which is attributed to the pressure-induced enlargement of the direct bandgap at the K point in the first Brillouin zone of MoS_2 where the A exciton is located. Accompanied by the shrinkage of the whole TA spectra along the vertical axis with the increase of the pressure, the seeming decrease of the negative bleaching peak eventually evolves into positive signals just like that shown in Fig. 2(b) under the pump fluence of 707 $\mu\mathrm{J}/\mathrm{cm}^2$. Meanwhile, the linewidth of the bleaching peak in the first three TA spectra remains almost unchanged under low pressures, which is in sharp contrast to the linewidth broadening under pressures above 1.81 GPa. The same variation tendency of the spectral features found in Figs. 3 and 2(b) (above the Mott threshold) are direct proof of the successful achievement of photoinduced Mott transition in few-layer MoS_2 under low excitation density via hydrostatic pressure. Besides, since the totally positive TA spectrum in Fig. 2(b) at ambient pressure can be only obtained under high pump fluence of 707 $\mu\mathrm{J}/\mathrm{cm}^2$, which corresponds to an excitation density ($4.7 \times 10^{14}/\mathrm{cm}^2$) of more than ten times of the Mott density ($4.2 \times 10^{13}/\mathrm{cm}^2$), thus the fixed excitation density of $3.29 \times 10^{12}/\mathrm{cm}^2$ should also be about ten times larger than the Mott density of the few-layer MoS_2 under pressures above 2.20 GPa, according to the spectral feature of totally positive TA signals. This suggests that the Mott density is at the $1 \times 10^{11}/\mathrm{cm}^2$ scale under pressures above 2.20 GPa. Thus, we can conclude that the Mott density of few-layer MoS_2 can be significantly reduced by more than two orders of magnitude via hydrostatic pressure of ~3 GPa.

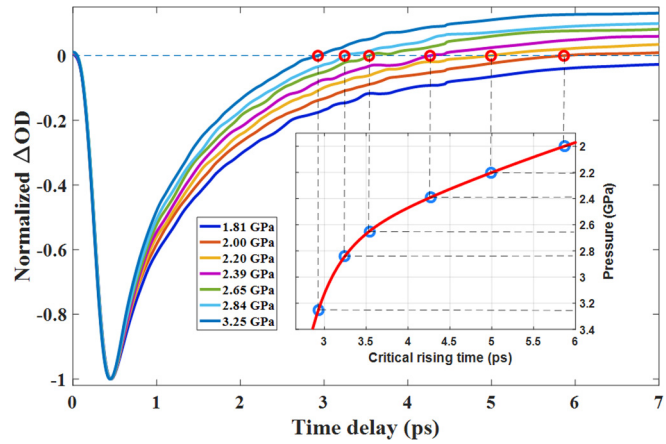

FIG. 4. TA traces of A exciton in few-layer MoS_2 under hydrostatic pressure from 1.81 to 3.25 GPa. The excitation density is fixed at $3.29 \times 10^{12}/\mathrm{cm}^2$. The evolution of the moment for the TA traces rising up across the zero baseline (horizontal blue dashed line), which is defined as the critical rising time, is presented as a function of the pressure in the inset and a red fitting curve is shown to guide to the eye.

To provide a further description of the ultrafast dynamics at the Mott transition under hydrostatic pressure, TA traces of A excitons are shown in Fig. 4 with the increase of the pressure from 1.81 to 3.25 GPa (as a direct visualization of the pressure-induced dynamic changes under conditions below and above the Mott threshold, the full TA spectra as a function of time delay and wavelength in false color together with TA slices at selected time delays in few-layer MoS_2 under pressure of 0.50 and 2.39 GPa are shown, respectively, in Figs. S7 and S8 in the Supplemental Material [48]). As shown in Fig. 4, the relaxation of the negative bleaching peak of A excitons gets faster and eventually rises up across the zero baseline within a shorter period of time on the picosecond timescale under elevated pressures. According to our previous study [46], the exciton relaxation dynamics in few-layer MoS_2 under hydrostatic pressure are dominated by the initial hot carrier cooling process within ~1 ps followed by the exciton dissociation with a lifetime of ~3–6 ps. On the one hand, it can be seen that the moments at which the TA traces of the exciton rising up across the zero baseline, which are defined as the critical rising time and marked with red circles in Fig. 4, fall exactly in the same time range of ~3–6 ps as the lifetime of the exciton dissociation. On the other hand,

as the TA traces were obtained via spectral integration over the A exciton bleaching peak, the sign reversal of the TA traces across the marked critical rising time is just another manifestation of the emergence of a totally positive A exciton signal as shown and discussed in Figs. 2 and 3, which has been assigned as the main spectral feature for the occurrence of photoinduced Mott transition. Thus, the critical rising time we defined here serves as a bridge that connects the exciton dissociation and the photoinduced Mott transition. Indeed, the free carriers originating from the dissociation of the excitons will in turn enhance the dynamical screening of the Coulomb interactions between electron-hole pairs and further facilitate the exciton fission, which contributes to the Mott transition from an insulating excitonic regime to a metallic electron-hole plasma phase.

Based on the above discussion, the underlying physical mechanism for the successful achievement of the Mott transition and the significant reduction of the Mott density under pressure with only mild excitation can be attributed to the reduced interlayer distance and the enhanced screening in few-layer MoS_2 under pressure, which then enhance the exciton dissociation and finally facilitate the photoinduced Mott transition. Actually, upon the compression strain from the hydrostatic pressure, the interlayer distance in few-layer MoS_2 can be readily reduced [41]. In previous studies, it has been verified that with the decrease of the interlayer distance in TMDCs, the Coulomb screening effects from adjacent layers will be enhanced, which result in the reduction of the exciton binding energy [63]. Together with the contributions from the photogenerated charge carriers to the dynamical screening of attractive Coulomb interactions between bound electron-hole pairs, exciton binding energy can be further reduced, which facilitates the exciton dissociation and significantly lowers the Mott threshold.

More importantly, since the critical rising time is directly related to the onset of the Mott transition, we can then use it as a quantitative parameter of the time needed for the ultrafast establishment of the metallic electron-hole plasma state after optical excitation. As shown in the inset of Fig. 4, with the increase of the pressure from 2.00 to 3.25 GPa, the critical rising time can be gradually reduced from ∼5.8 to 2.9 ps. Furthermore, as shown in Fig. S9 (see Fig. S9 in the Supplemental Material [48]), the transition rate corresponding to the reciprocal of the critical rising time increases as a linear function of the pressure up to 3 GPa. These findings reveal unambiguously that the ultrafast optical switching to the metallic state in few-layer MoS_2 can be subtly tuned and accelerated via the hydrostatic pressure with a subpicosecond time resolution. As shown by the red fitting curve in the inset of Fig. 4, the critical rising time evolves nonlinearly with the pressure under the fixed low excitation density. This nonlinear behavior indicates that the switching to the metallic state can be manipulated with much higher time resolution under higher pressures, which may find promising applications in strain-tunable ultrafast optical switches and phototransistors.

III. CONCLUSION

In summary, we have experimentally demonstrated that the photoinduced Mott transition in few-layer MoS_2 under mild excitation density can be successfully achieved and subtly tuned via hydrostatic pressure at room temperature. Utilizing the strategy of combining ultrafast pump-probe spectroscopy with DAC devices, we find that the Mott density of few-layer MoS_2 under pressure of ∼3 GPa can be significantly reduced by more than two orders of magnitude compared with that at ambient pressure. Besides, with the increase of the pressure from 2.00 to 3.25 GPa, the time needed for the ultrafast optical switching to a metallic state in few-layer MoS_2 after excitation can be successively reduced from ∼5.8 to 2.9 ps, which is attributed to the reduction of the exciton binding energy and the acceleration of the exciton dissociation by the enhanced dielectric screening of the Coulomb interactions with the pressure. Our findings enrich the understanding of many-body interactions in atomically thin TMDCs under external strain, which may facilitate their promising applications in next-generation 2D-based phototransistors, strain-tunable ultrafast optical switches, and energy-efficient nanolasers. Meanwhile, the proposed strategy with the combination of ultrafast pump-probe spectroscopy with DAC devices is versatile and powerful, which paves the way for the study of strong-correlation effects and macroscopic quantum phenomena like Bose-Einstein condensation [11,64] in solids under extreme conditions.

ACKNOWLEDGMENTS

We acknowledge support from the National Key Research and Development Program (No. 2019YFA0307701), the National Natural Science Foundation of China (NSFC No. 11974138). The experimental work was supported by the Strategic Priority Research Program of the Chinese Academy of Sciences (Grant No. XDB17000000), the Chemical Dynamics Research Center (Grant No. 21688102), the international partnership program of Chinese Academy of Sciences (No. 121421KYSB20170012), and the Key Technology Team of the Chinese Academy of Sciences (Grant No. GJJSTD20190002).

[1] H. Haug and S. W. Koch, Quantum Theory of the Optical and Electronic Properties of Semiconductors, 5th ed. (World Scientific, Singapore, 2009).

[2] M. Z. Maialle, E. A. de Andrada e Silva, and L. J. Sham, Exciton spin dynamics in quantum wells, Phys. Rev. B **47**, 15776 (1993).

[3] J. Szczytko, L. Kappei, J. Berney, F. Morier-Genoud, M. T. Portella-Oberli, and B. Deveaud, Determination of the Exciton Formation in Quantum Wells from Time-Resolved Interband Luminescence, Phys. Rev. Lett. **93**, 137401 (2004).

[4] A. L. Efros, M. Rosen, M. Kuno, M. Nirmal, D. J. Norris, and M. Bawendi, Band-edge exciton in quantum dots of semiconductors with a degenerate valence band: Dark and bright exciton states, Phys. Rev. B **54**, 4843 (1996).

[5] J. Heckötter, M. Freitag, D. Fröhlich, M. Aßmann, M. Bayer, P. Grünwald, F. Schöne, D. Semkat, H. Stolz, and S. Scheel,

Rydberg Excitons in the Presence of an Ultralow-Density Electron-Hole Plasma, Phys. Rev. Lett. **121**, 097401 (2018).

[6] A. Hangleiter, Z. Jin, M. Gerhard, D. Kalincev, T. Langer, H. Bremers, U. Rossow, M. Koch, M. Bonn, and D. Turchinovich, Efficient formation of excitons in a dense electron-hole plasma at room temperature, Phys. Rev. B **92**, 241305(R) (2015).

[7] E. Hendry, M. Koeberg, and M. Bonn, Exciton and electron-hole plasma formation dynamics in ZnO, Phys. Rev. B **76**, 045214 (2007).

[8] L. Kappei, J. Szczytko, F. Morier-Genoud, and B. Deveaud, Direct Observation of the Mott Transition in an Optically Excited Semiconductor Quantum Well, Phys. Rev. Lett. **94**, 147403 (2005).

[9] S. Iwai, M. Ono, A. Maeda, H. Matsuzaki, H. Kishida, H. Okamoto, and Y. Tokura, Ultrafast Optical Switching to a Metallic State by Photoinduced Mott Transition in a Halogen-Bridged Nickel-Chain Compound, Phys. Rev. Lett. **91**, 057401 (2003).

[10] M. Stern, V. Garmider, V. Umansky, and I. Bar-Joseph, Mott Transition of Excitons in Coupled Quantum Wells, Phys. Rev. Lett. **100**, 256402 (2008).

[11] D. Semkat, F. Richter, D. Kremp, G. Manzke, W.-D. Kraeft, and K. Henneberger, Ionization equilibrium in an excited semiconductor: Mott transition versus Bose-Einstein condensation, Phys. Rev. B **80**, 155201 (2009).

[12] A. Steinhoff, M. Florian, M. Rösner, G. Schönhoff, T. O. Wehling, and F. Jahnke, Exciton fission in monolayer transition metal dichalcogenide semiconductors, Nat. Commun. **8**, 1166 (2017).

[13] Q. H. Wang, K. Kalantar-Zadeh, A. Kis, J. N. Coleman, and M. S. Strano, Electronics and optoelectronics of two-dimensional transition metal dichalcogenides, Nat. Nanotechnol. **7**, 699 (2012).

[14] M. Chhowalla, H. S. Shin, G. Eda, L.-J. Li, K. P. Loh, and H. Zhang, The chemistry of two-dimensional layered transition metal dichalcogenide nanosheets, Nat. Chem. **5**, 263 (2013).

[15] K. F. Mak, C. Lee, J. Hone, J. Shan, and T. F. Heinz, Atomically Thin MoS_2: A New Direct-Gap Semiconductor, Phys. Rev. Lett. **105**, 136805 (2010).

[16] A. Chernikov, T. C. Berkelbach, H. M. Hill, A. Rigosi, Y. Li, O. B. Aslan, D. R. Reichman, M. S. Hybertsen, and T. F. Heinz, Exciton Binding Energy and Nonhydrogenic Rydberg Series in Monolayer WS_2, Phys. Rev. Lett. **113**, 076802 (2014).

[17] K. He, N. Kumar, L. Zhao, Z. Wang, K. F. Mak, H. Zhao, and J. Shan, Tightly Bound Excitons in Monolayer WSe_2, Phys. Rev. Lett. **113**, 026803 (2014).

[18] H. M. Hill, A. F. Rigosi, C. Roquelet, A. Chernikov, T. C. Berkelbach, D. R. Reichman, M. S. Hybertsen, L. E. Brus, and T. F. Heinz, Observation of excitonic Rydberg states in monolayer MoS_2 and WS_2 by photoluminescence excitation spectroscopy, Nano Lett. **15**, 2992 (2015).

[19] A. Chernikov, A. M. van der Zande, H. M. Hill, A. F. Rigosi, A. Velauthapillai, J. Hone, and T. F. Heinz, Electrical Tuning of Exciton Binding Energies in Monolayer WS_2, Phys. Rev. Lett. **115**, 126802 (2015).

[20] A. Splendiani, L. Sun, Y. Zhang, T. Li, J. Kim, C.-Y. Chim, G. Galli, and F. Wang, Emerging photoluminescence in monolayer MoS_2, Nano Lett. **10**, 1271 (2010).

[21] C. Ruppert, A. Chernikov, H. M. Hill, A. F. Rigosi, and T. F. Heinz, The role of electronic and phononic excitation in the optical response of monolayer WS_2 after ultrafast excitation, Nano Lett. **17**, 644 (2017).

[22] R. Wang, B. A. Ruzicka, N. Kumar, M. Z. Bellus, H.-Y. Chiu, and H. Zhao, Ultrafast and spatially resolved studies of charge carriers in atomically thin molybdenum disulfide, Phys. Rev. B **86**, 045406 (2012).

[23] H. Shi, R. Yan, S. Bertolazzi, J. Brivio, B. Gao, A. Kis, D. Jena, H. G. Xing, and L. Huang, Exciton dynamics in suspended monolayer and few-layer MoS_2 2D crystals, ACS Nano **7**, 1072 (2013).

[24] D. Kozawa, R. Kumar, A. Carvalho, K. Kumar Amara, W. Zhao, S. Wang, M. Toh, R. M. Ribeiro, A. H. Castro Neto, K. Matsuda, and G. Eda, Photocarrier relaxation pathway in two-dimensional semiconducting transition metal dichalcogenides, Nat. Commun. **5**, 4543 (2014).

[25] E. J. Sie, A. J. Frenzel, Y.-H. Lee, J. Kong, and N. Gedik, Intervalley biexcitons and many-body effects in monolayer MoS_2, Phys. Rev. B **92**, 125417 (2015).

[26] D. Sun, Y. Rao, G. A. Reider, G. Chen, Y. You, L. BrÃ©zin, A. R. Harutyunyan, and T. F. Heinz, Observation of rapid exciton-exciton annihilation in monolayer molybdenum disulfide, Nano Lett. **14**, 5625 (2014).

[27] A. Chernikov, C. Ruppert, H. M. Hill, A. F. Rigosi, and T. F. Heinz, Population inversion and giant bandgap renormalization in atomically thin WS_2 layers, Nat. Photonics **9**, 466 (2015).

[28] S. Wu, S. Buckley, J. R. Schaibley, L. Feng, J. Yan, D. G. Mandrus, F. Hatami, W. Yao, J. Vučković, A. Majumdar, and X. Xu, Monolayer semiconductor nanocavity lasers with ultralow thresholds, Nature (London) **520**, 69 (2015).

[29] Y. Ye, Z. J. Wong, X. Lu, X. Ni, H. Zhu, X. Chen, Y. Wang, and X. Zhang, Monolayer excitonic laser, Nat. Photonics **9**, 733 (2015).

[30] K. Asano and T. Yoshioka, Exciton-Mott physics in two-dimensional electron-hole systems: Phase diagram and single-particle spectra, J. Phys. Soc. Jpn. **83**, 084702 (2014).

[31] Z. Wang, H. Sun, Q. Zhang, J. Feng, J. Zhang, Y. Li, and C.-Z. Ning, Excitonic complexes and optical gain in two-dimensional molybdenum ditelluride well below the Mott transition, Light Sci Appl **9**, 39 (2020).

[32] B. Radisavljevic and A. Kis, Mobility engineering and a metal-insulator transition in monolayer MoS_2, Nat. Mater. **12**, 815 (2013).

[33] F. Yu, Q. Liu, X. Gan, M. Hu, T. Zhang, C. Li, F. Kang, M. Terrones, and R. Lv, Ultrasensitive pressure detection of few-layer MoS_2, Adv. Mater. **29**, 1603266 (2017).

[34] S. Bertolazzi, J. Brivio, and A. Kis, Stretching and breaking of ultrathin MoS_2, ACS Nano **5**, 9703 (2011).

[35] A. San-Miguel, Nanomaterials under high-pressure, Chem. Soc. Rev. **35**, 876 (2006).

[36] H.-K. Mao, B. Chen, J. Chen, K. Li, J.-F. Lin, W. Yang, and H. Zheng, Recent advances in high-pressure science and technology, Matter Radiat. Extr. **1**, 59 (2016).

[37] A. P. Nayak, S. Bhattacharyya, J. Zhu, J. Liu, X. Wu, T. Pandey, C. Jin, A. K. Singh, D. Akinwande, and J.-F. Lin, Pressure-induced semiconducting to metallic transition in multilayered molybdenum disulphide, Nat. Commun. **5**, 3731 (2014).

[38] C.-H. Chang, X. Fan, S.-H. Lin, and J.-L. Kuo, Orbital analysis of electronic structure and phonon dispersion in MoS_2, $MoSe_2$,

WS_2, and WSe_2 monolayers under strain, Phys. Rev. B **88**, 195420 (2013).

[39] Z.-H. Chi, X.-M. Zhao, H. Zhang, A. F. Goncharov, S. S. Lobanov, T. Kagayama, M. Sakata, and X.-J. Chen, Pressure-Induced Metallization of Molybdenum Disulfide, Phys. Rev. Lett. **113**, 036802 (2014).

[40] X. Dou, K. Ding, D. Jiang, and B. Sun, Tuning and identification of interband transitions in monolayer and bilayer molybdenum disulfide using hydrostatic pressure, ACS Nano **8**, 7458 (2014).

[41] X. Dou, K. Ding, D. Jiang, X. Fan, and B. Sun, Probing spin-orbit coupling and interlayer coupling in atomically thin molybdenum disulfide using hydrostatic pressure, ACS Nano **10**, 1619 (2016).

[42] Y. Chen, F. Ke, P. Ci, C. Ko, T. Park, S. Saremi, H. Liu, Y. Lee, J. Suh, L. W. Martin, J. W. Ager, B. Chen, and J. Wu, Pressurizing field-effect transistors of few-layer MoS_2 in a diamond anvil cell, Nano Lett. **17**, 194 (2017).

[43] P. Ci, Y. Chen, J. Kang, R. Suzuki, H. S. Choe, J. Suh, C. Ko, T. Park, K. Shen, Y. Iwasa, S. Tongay, J. W. Ager, L.-W. Wang, and J. Wu, Quantifying van der Waals interactions in layered transition metal dichalcogenides from pressure-enhanced valence band splitting, Nano Lett. **17**, 4982 (2017).

[44] Z. Zhao, H. Zhang, H. Yuan, S. Wang, Y. Lin, Q. Zeng, G. Xu, Z. Liu, G. K. Solanki, K. D. Patel, Y. Cui, H. Y. Hwang, and W. L. Mao, Pressure induced metallization with absence of structural transition in layered molybdenum diselenide, Nat. Commun. **6**, 7312 (2015).

[45] A. P. Nayak, Z. Yuan, B. Cao, J. Liu, J. Wu, S. T. Moran, T. Li, D. Akinwande, C. Jin, and J.-F. Lin, Pressure-modulated conductivity, carrier density, and mobility of multilayered tungsten disulfide, ACS Nano **9**, 9117 (2015).

[46] Q. Li, L. Sui, G. Niu, J. Jiang, Y. Zhang, G. Wu, M. Jin, and K. Yuan, Pressure manipulation of interlayer interactions and ultrafast carrier dynamics in few-layer MoS_2, J. Phys. Chem. C **124**, 11183 (2020).

[47] J. N. Coleman, M. Lotya, A. O'Neill, S. D. Bergin, P. J. King, U. Khan, K. Young, A. Gaucher, S. De, R. J. Smith, I. V. Shvets, S. K. Arora, G. Stanton, H.-Y. Kim, K. Lee, G. T. Kim, G. S. Duesberg, T. Hallam, J. J. Boland, J. J. Wang, J. F. Donegan, J. C. Grunlan, G. Moriarty, A. Shmeliov, R. J. Nicholls, J. M. Perkins, E. M. Grieveson, K. Theuwissen, D. W. McComb, P. D. Nellist, and V. Nicolosi, Two-dimensional nanosheets produced by liquid exfoliation of layered materials, Science **331**, 568 (2011).

[48] See Supplemental Material at http://link.aps.org/supplemental/10.1103/PhysRevB.103.125416 for detailed experimental setup, including the sample preparation, DAC device loading, and the steady-state and TA spectroscopy setup under hydrostatic pressure, together with additional experimental results especially for series of TA spectra .

[49] E. J. Sie, A. Steinhoff, C. Gies, C. H. Lui, Q. Ma, M. Rösner, G. Schönhoff, F. Jahnke, T. O. Wehling, Y.-H. Lee, J. Kong, P. Jarillo-Herrero, and N. Gedik, Observation of exciton redshift-blueshift crossover in monolayer WS_2, Nano Lett. **17**, 4210 (2017).

[50] G. Wang, A. Chernikov, M. M. Glazov, T. F. Heinz, X. Marie, T. Amand, and B. Urbaszek, Colloquium: Excitons in atomically thin transition metal dichalcogenides, Rev. Mod. Phys. **90**, 021001 (2018).

[51] P. D. Cunningham, A. T. Hanbicki, K. M. McCreary, and B. T. Jonker, Photoinduced bandgap renormalization and exciton binding energy reduction in WS_2, ACS Nano **11**, 12601 (2017).

[52] M. M. Ugeda, A. J. Bradley, S.-F. Shi, F. H. da Jornada, Y. Zhang, D. Y. Qiu, W. Ruan, S.-K. Mo, Z. Hussain, Z.-X. Shen, F. Wang, S. G. Louie, and M. F. Crommie, Giant bandgap renormalization and excitonic effects in a monolayer transition metal dichalcogenide semiconductor, Nat. Mater. **13**, 1091 (2014).

[53] E. A. A. Pogna, M. Marsili, D. De Fazio, S. Dal Conte, C. Manzoni, D. Sangalli, D. Yoon, A. Lombardo, A. C. Ferrari, A. Marini, G. Cerullo, and D. Prezzi, Photo-induced bandgap renormalization governs the ultrafast response of single-layer MoS_2, ACS Nano **10**, 1182 (2016).

[54] G. Kime, M. A. Leontiadou, J. R. Brent, N. Savjani, P. O'Brien, and D. Binks, Ultrafast charge dynamics in dispersions of monolayer MoS_2 nanosheets, J. Phys. Chem. C **121**, 22415 (2017).

[55] L. Wibmer, S. Lages, T. Unruh, and D. M. Guldi, Excitons and trions in one-photon- and two-photon-excited MoS_2: A study in dispersions, Adv. Mater. **30**, 1706702 (2018).

[56] K. F. Mak, K. He, C. Lee, G. H. Lee, J. Hone, T. F. Heinz, and J. Shan, Tightly bound trions in monolayer MoS_2, Nat. Mater. **12**, 207 (2013).

[57] C.-K. Yong, J. Horng, Y. Shen, H. Cai, A. Wang, C.-S. Yang, C.-K. Lin, S. Zhao, K. Watanabe, T. Taniguchi, S. Tongay, and F. Wang, Biexcitonic optical stark effects in monolayer molybdenum diselenide, Nat. Phys. **14**, 1092 (2018).

[58] A. Steinhoff, M. Florian, A. Singh, K. Tran, M. Kolarczik, S. Helmrich, A. W. Achtstein, U. Woggon, N. Owschimikow, F. Jahnke, and X. Li, Biexciton fine structure in monolayer transition metal dichalcogenides, Nat. Phys. **14**, 1199 (2018).

[59] C. F. Klingshirn, *Semiconductor Optics*, 4th ed. (Springer-Verlag, Berlin, 2012).

[60] T. Suzuki and R. Shimano, Time-Resolved Formation of Excitons and Electron-Hole Droplets in Si Studied Using Terahertz Spectroscopy, Phys. Rev. Lett. **103**, 057401 (2009).

[61] Q. Zhang, Y. Wang, W. Gao, Z. Long, J. D. Watson, M. J. Manfra, A. Belyanin, and J. Kono, Stability of High-Density Two-Dimensional Excitons Against a Mott Transition in High Magnetic Fields Probed by Coherent Terahertz Spectroscopy, Phys. Rev. Lett. **117**, 207402 (2016).

[62] F. Sekiguchi, T. Mochizuki, C. Kim, H. Akiyama, L. N. Pfeiffer, K. W. West, and R. Shimano, Anomalous Metal Phase Emergent on the Verge of an Exciton Mott Transition, Phys. Rev. Lett. **118**, 067401 (2017).

[63] M. Florian, M. Hartmann, A. Steinhoff, J. Klein, A. W. Holleitner, J. J. Finley, T. O. Wehling, M. Kaniber, and C. Gies, The dielectric impact of layer distances on exciton and trion binding energies in van der Waals heterostructures, Nano Lett. **18**, 2725 (2018).

[64] J. Kasprzak, M. Richard, S. Kundermann, A. Baas, P. Jeambrun, J. M. J. Keeling, F. M. Marchetti, M. H. Szymańska, R. André, J. L. Staehli, V. Savona, P. B. Littlewood, B. Deveaud, and L. S. Dang, Bose-Einstein condensation of exciton polaritons, Nature (London) **443**, 409 (2006).